Study of Interstitial Oxygen Near Surface of Mid-T Heat-Treated Nb SRF Cavities: Frequency Shift Analysis

Rezvan Ghanbari

on behalf of SRF R&D team

4 December 2025

Medium Temperature (Mid-T) Heat Treatment

different recipes at 200-400°C for 3-20 hours in UHV

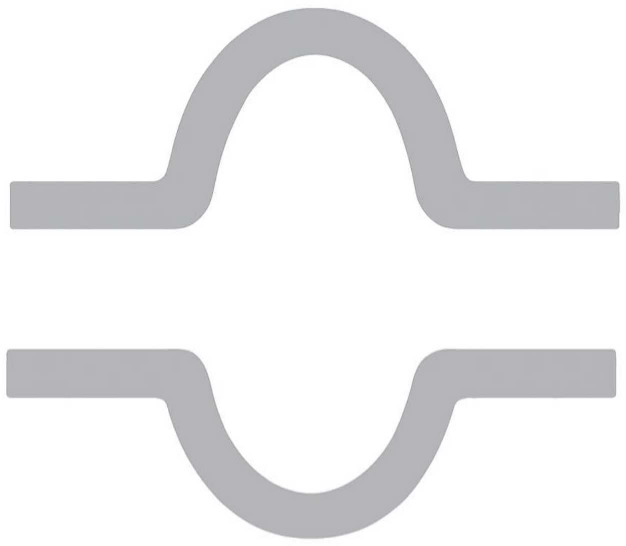

Medium Temperature (Mid-T) Heat Treatment

different recipes at 200-400°C for 3-20 hours in UHV

- Nb_2O_5 dissociation begins at 200–250 °C, whereas other oxide layers require higher temperatures

[M. Delheusy, 2008, X-ray investigation of Nb/O interfaces]

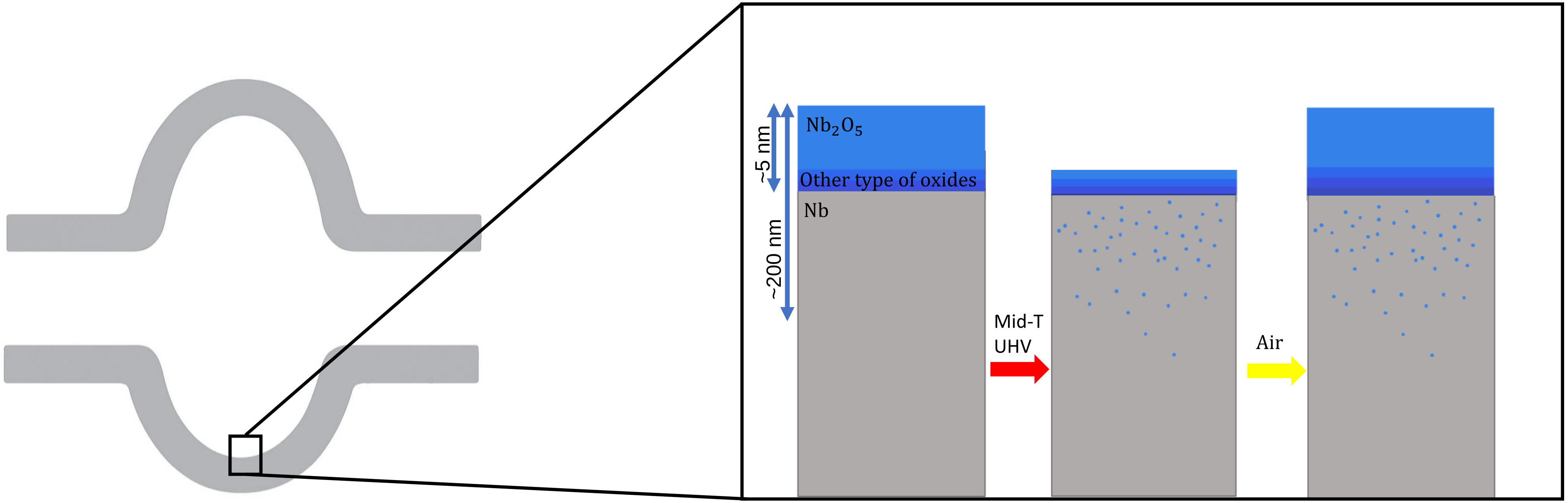

Resonance Frequency Shift Measurement

a non-invasive method to probe interstitial oxygen in the near-surface of cavities

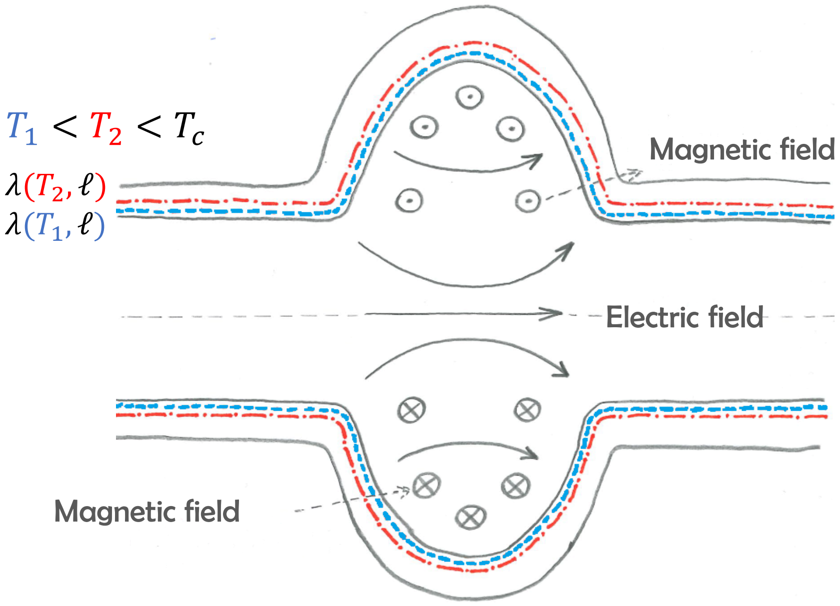

$$\frac{\Delta f}{f} = -\frac{f \mu_0 \Delta\lambda}{2G}$$

Resonance Frequency Shift Measurement

a non-invasive method to probe interstitial oxygen in the near-surface of cavities

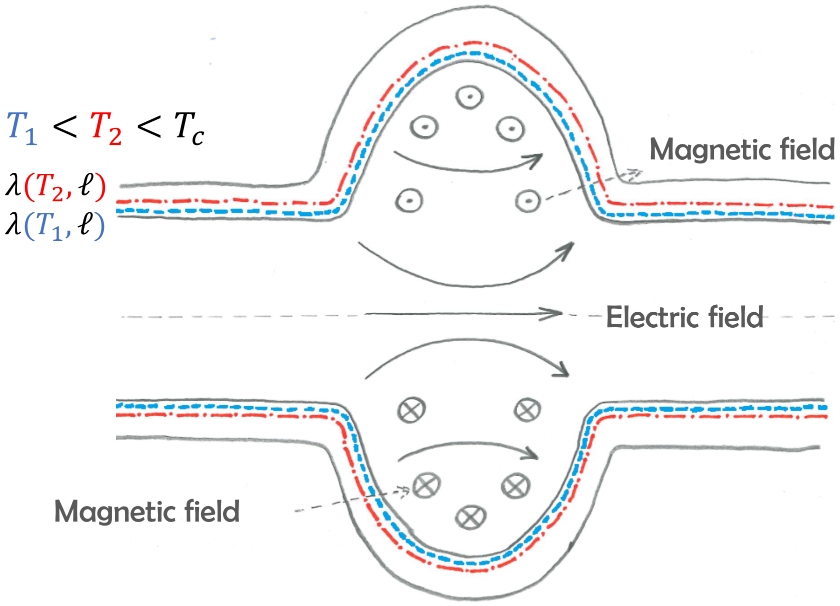

$$\frac{\Delta f}{f} = -\frac{f \mu_0 \Delta\lambda}{2G}$$

✓ Interstitial oxygen acts as a scattering center in niobium and modifies the electron mean free path

Resonance Frequency Shift Measurement

a non-invasive method to probe interstitial oxygen in the near-surface of cavities

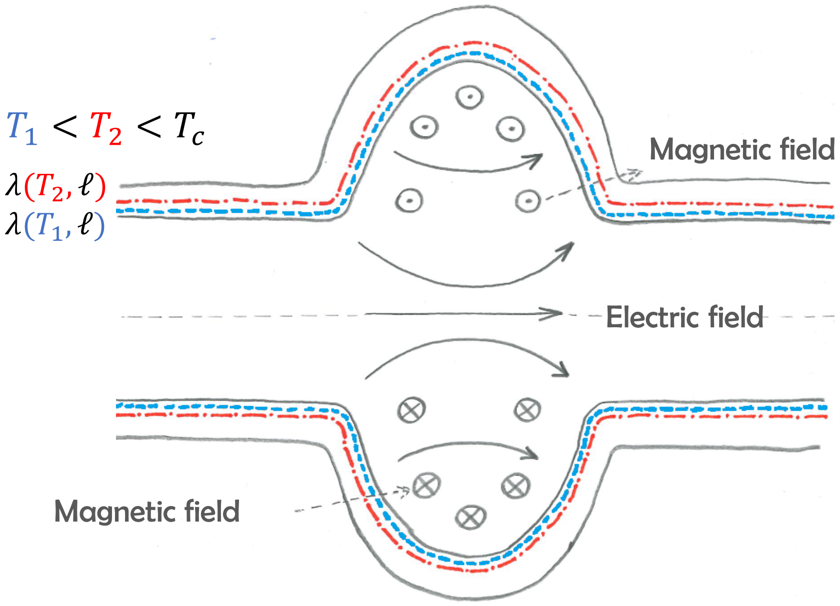

$$\frac{\Delta f}{f} = -\frac{f \mu_0 \Delta\lambda}{2G}$$

- ✓ Interstitial oxygen acts as a scattering center in niobium and modifies the electron mean free path
- ✓ The mean free path governs RF behavior in both the superconducting and normal-conducting states

Resonance Frequency Shift Measurement

a non-invasive method to probe interstitial oxygen in the near-surface of cavities

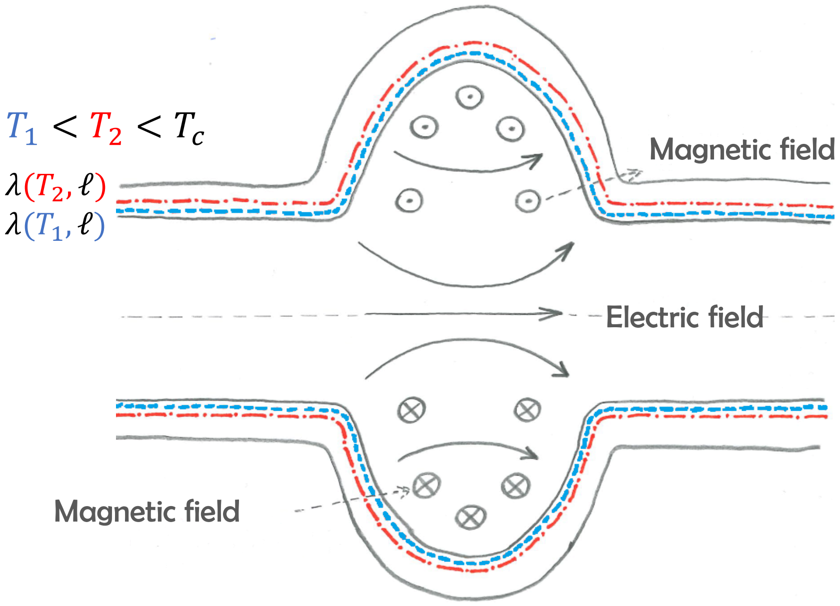

$$\frac{\Delta f}{f} = -\frac{f \mu_0 \Delta\lambda}{2G}$$

- ✓ Interstitial oxygen acts as a scattering center in niobium and modifies the electron mean free path
- ✓ The mean free path governs RF behavior in both the superconducting and normal-conducting states
- ✓ Differences in mean free path produce a measurable imprint on the resonant frequency

Resonance Frequency Shift Measurement

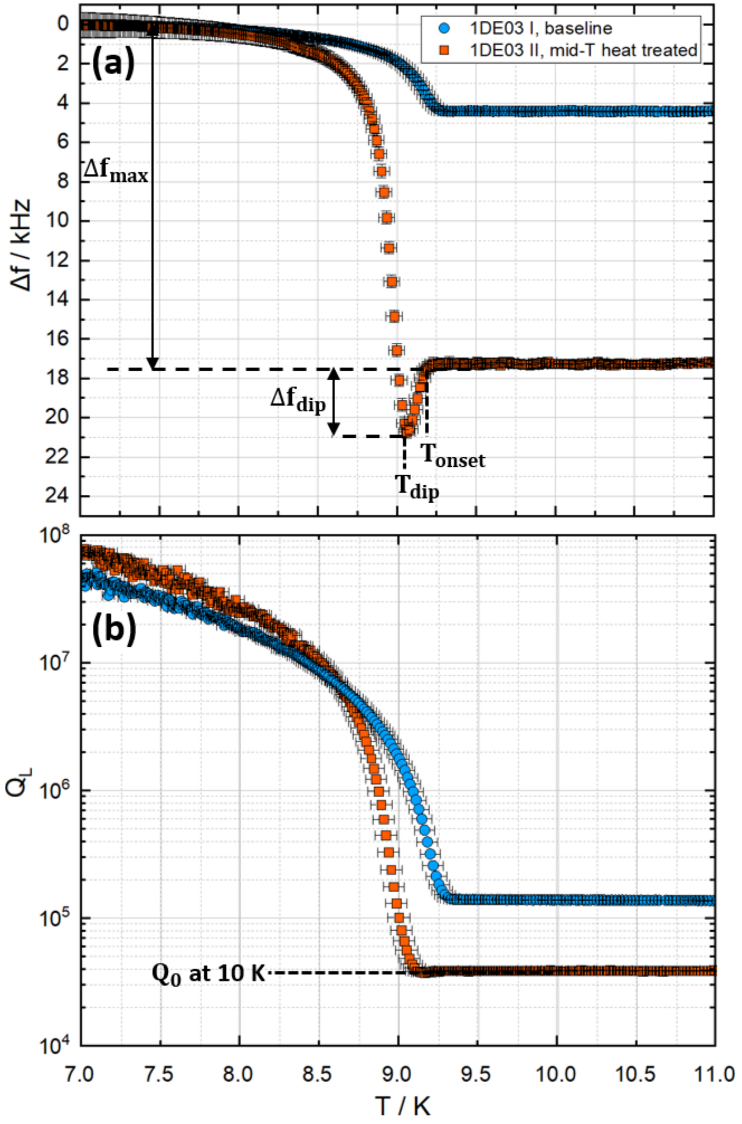

Resonance Frequency Shift Measurement

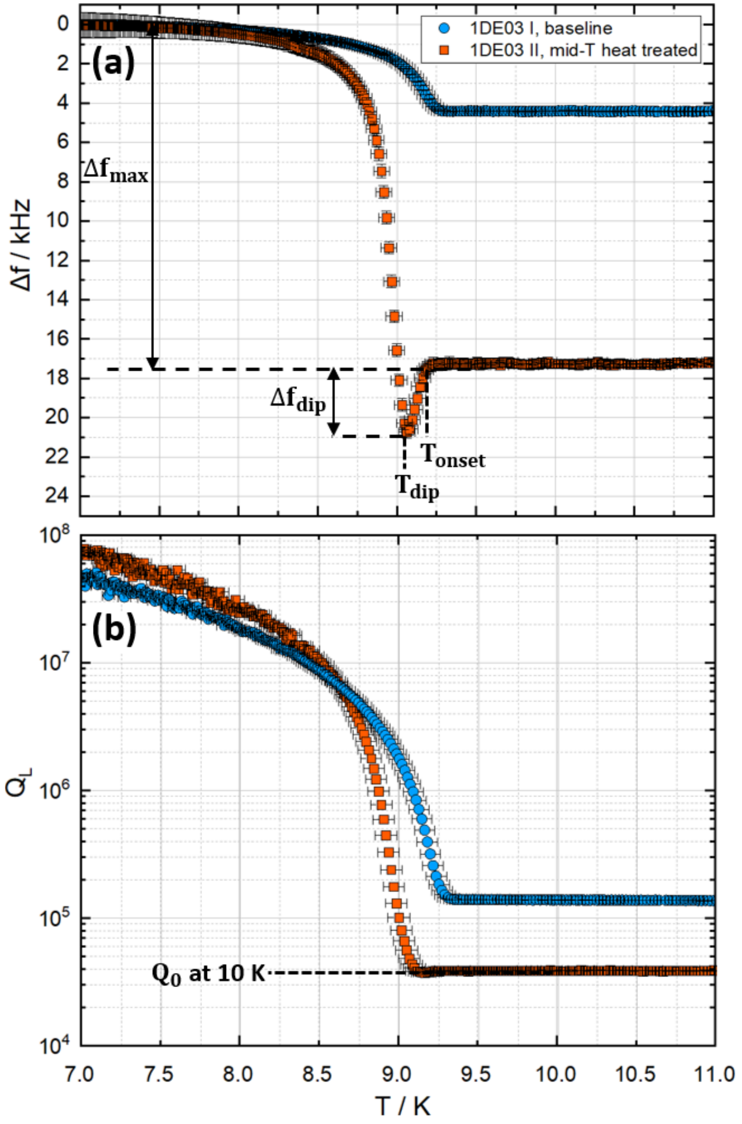

- $$\frac{\Delta f}{f} = -\frac{f\mu_0\Delta\lambda}{2G},$$
  $$\lambda(T) = \frac{\lambda_0}{\sqrt{1-\left(\frac{T}{T_c}\right)^4}}, \lambda_0 = \lambda_L\sqrt{1+\frac{\pi\xi_0}{2\ell}}$$

Resonance Frequency Shift Measurement

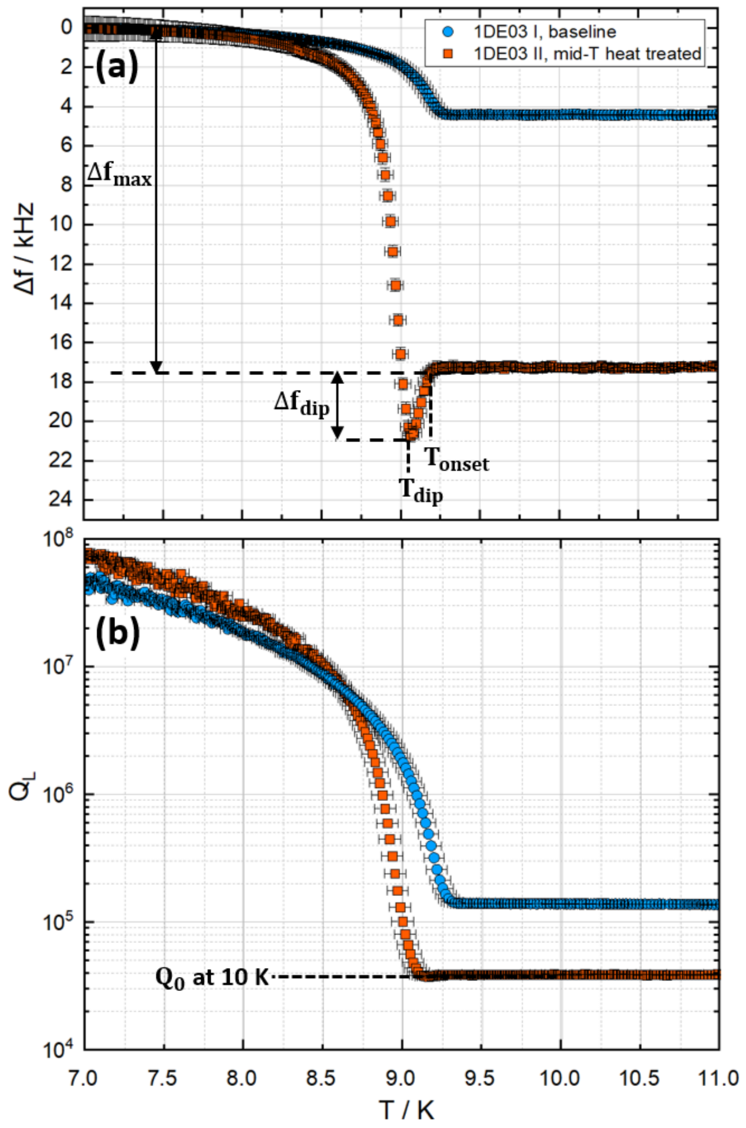

- $$\frac{\Delta f}{f} = -\frac{f\mu_0\Delta\lambda}{2G},$$
  $$\lambda(T) = \frac{\lambda_0}{\sqrt{1-\left(\frac{T}{T_c}\right)^4}}, \lambda_0 = \lambda_L\sqrt{1+\frac{\pi\xi_0}{2\ell}}$$

→

The total penetration depth	$\Delta\lambda_{max}$
The average mean free path within the total penetration depth	ℓ_λ

Resonance Frequency Shift Measurement

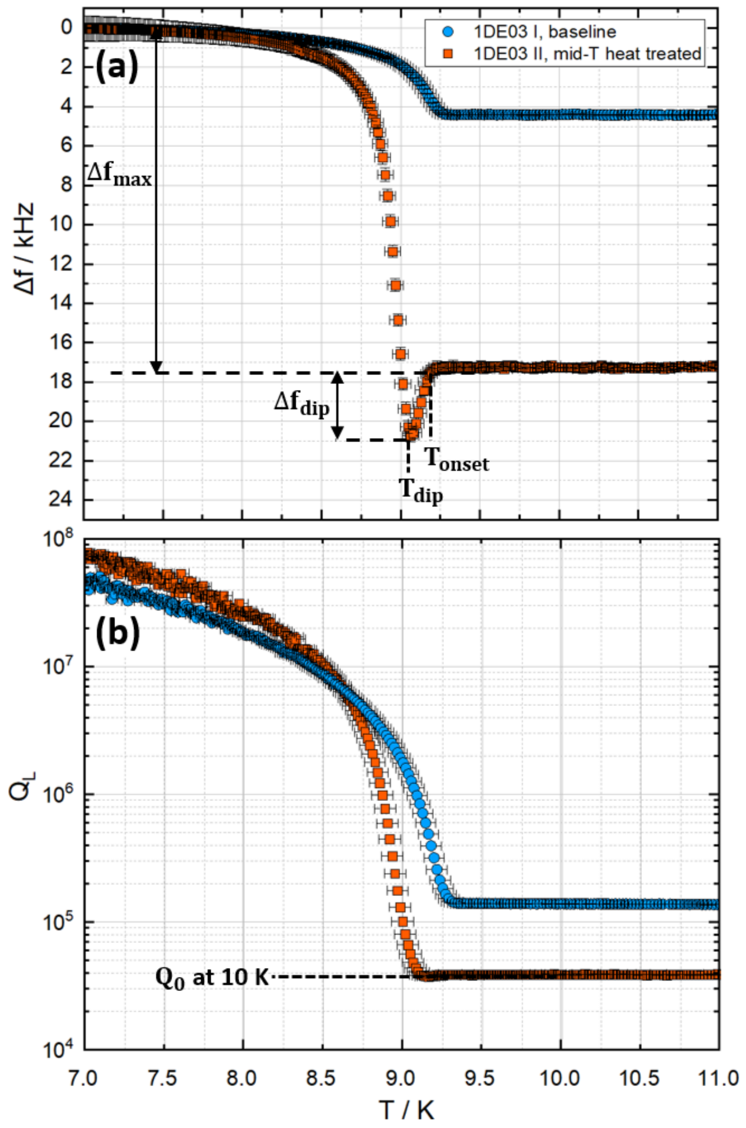

- $\frac{\Delta f}{f} = -\frac{f\mu_0 \Delta\lambda}{2G}$,
  $\lambda(T) = \frac{\lambda_0}{\sqrt{1-\left(\frac{T}{T_c}\right)^4}}$, $\lambda_0 = \lambda_L \sqrt{1+\frac{\pi\xi_0}{2\ell}}$ →

The total penetration depth	$\Delta\lambda_{max}$
The average mean free path within the total penetration depth	ℓ_λ

- Dip phenomenon

Resonance Frequency Shift Measurement

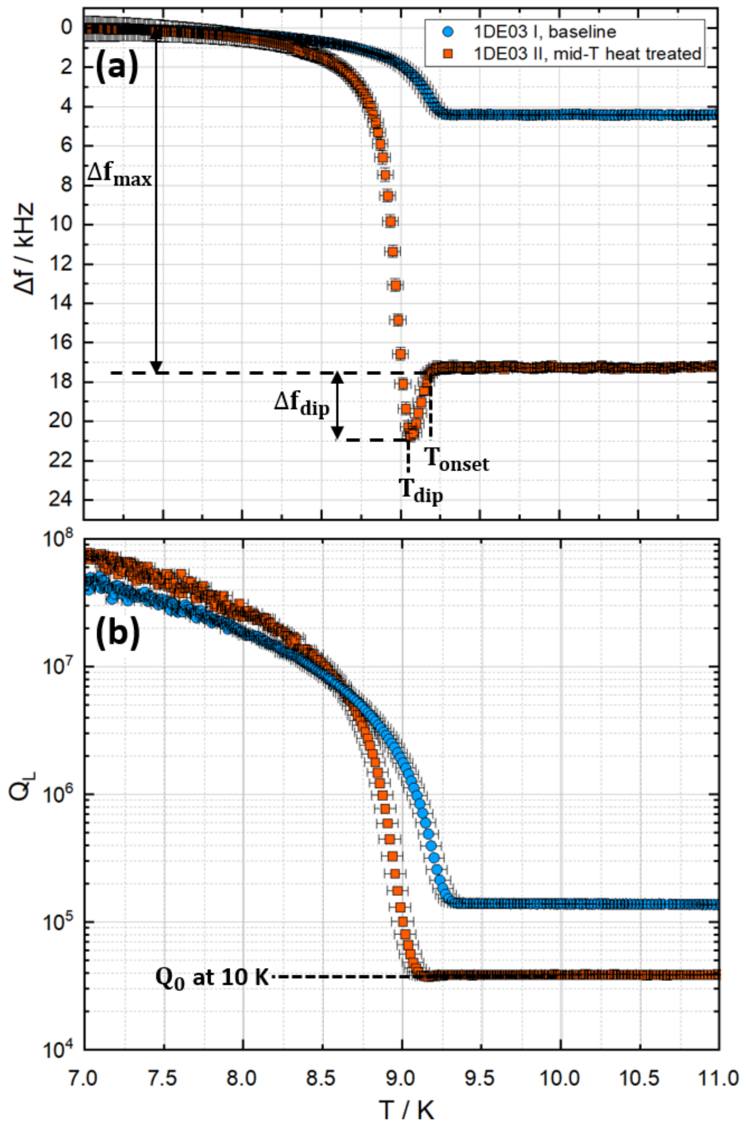

- $\frac{\Delta f}{f} = -\frac{f \mu_0 \Delta\lambda}{2G}$,
  $\lambda(T) = \frac{\lambda_0}{\sqrt{1-\left(\frac{T}{T_c}\right)^4}}$, $\lambda_0 = \lambda_L \sqrt{1 + \frac{\pi \xi_0}{2\ell}}$ →
- Dip phenomenon →

The total penetration depth	$\Delta\lambda_{max}$
The average mean free path within the total penetration depth	ℓ_λ
The dip magnitude	Δf_{dip}
The dip width	$T_{onset} - T_{dip}$

Resonance Frequency Shift Measurement

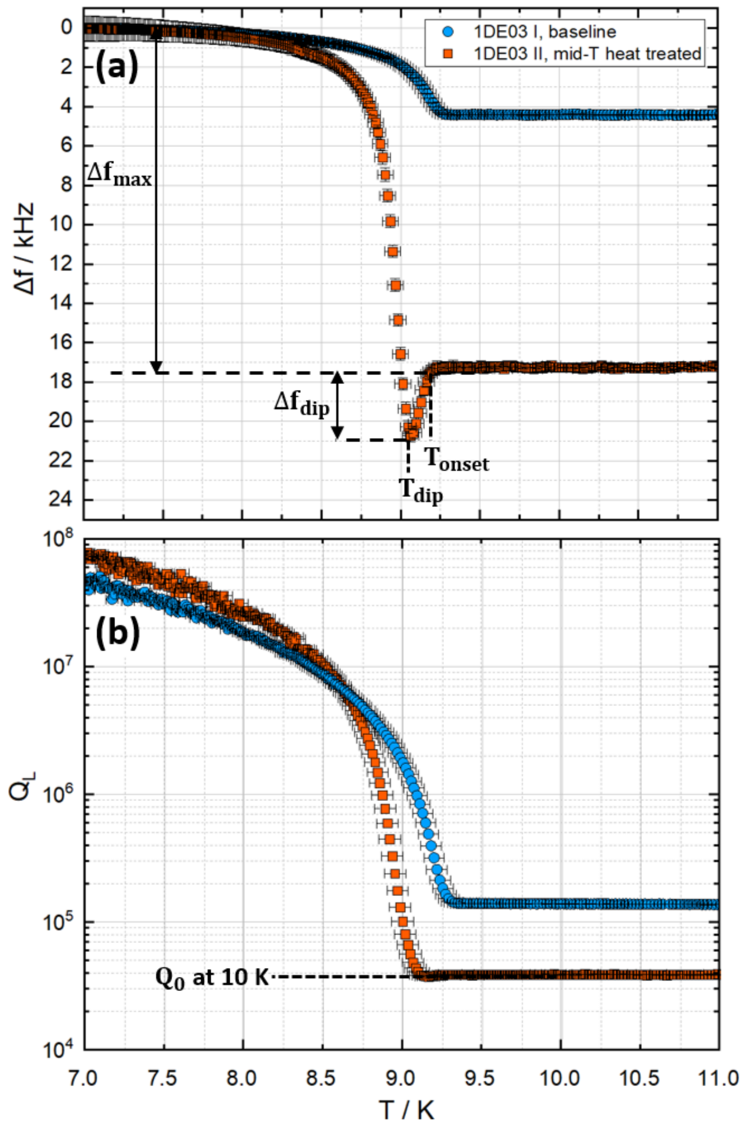

- $$\frac{\Delta f}{f} = -\frac{f\mu_0\Delta\lambda}{2G},$$
  $$\lambda(T) = \frac{\lambda_0}{\sqrt{1-\left(\frac{T}{T_c}\right)^4}}, \lambda_0 = \lambda_L\sqrt{1+\frac{\pi\xi_0}{2\ell}}$$

  →

- Dip phenomenon →

The total penetration depth	$\Delta\lambda_{max}$
The average mean free path within the total penetration depth	ℓ_λ
The dip magnitude	Δf_{dip}
The dip width	$T_{onset} - T_{dip}$

- $$Q_0 = \frac{G}{R_s}, Q_0(10\ K) \cong Q_L(10\ K),$$
  $$\rho\ell_{Nb} = 3.7 \times 10^{-16}\ \Omega m^2$$

[E. L. Garwin, et al., 1972, Resistivity Ratio of Niobium Superconducting Cavities]

Resonance Frequency Shift Measurement

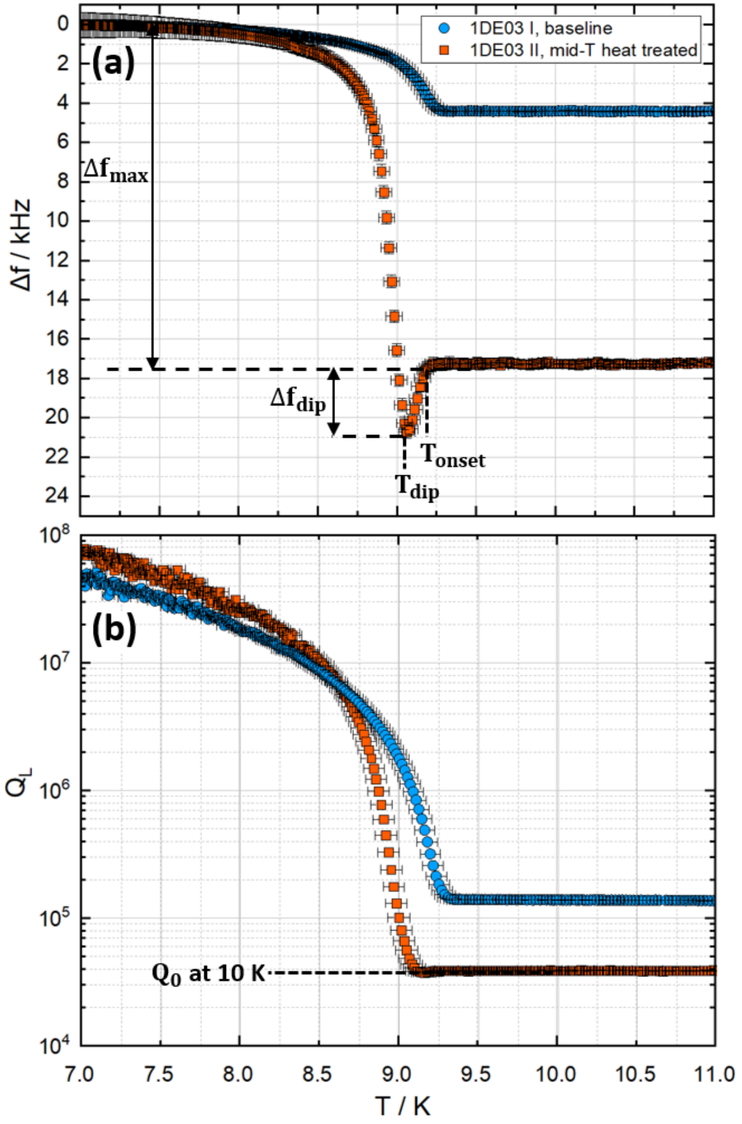

- $\frac{\Delta f}{f} = -\frac{f \mu_0 \Delta\lambda}{2G}$,
  $\lambda(T) = \frac{\lambda_0}{\sqrt{1-\left(\frac{T}{T_c}\right)^4}}, \lambda_0 = \lambda_L \sqrt{1+\frac{\pi\xi_0}{2\ell}}$ →
- Dip phenomenon →
- $Q_0 = \frac{G}{R_s}, Q_0(10\ K) \cong Q_L(10\ K)$,
  $\rho\ell_{Nb} = 3.7 \times 10^{-16}\ \Omega m^2$ →
  [E. L. Garwin, et al., 1972, Resistivity Ratio of Niobium Superconducting Cavities]

The total penetration depth	$\Delta\lambda_{max}$
The average mean free path within the total penetration depth	ℓ_λ
The dip magnitude	Δf_{dip}
The dip width	$T_{onset} - T_{dip}$
The normal conducting skin depth	δ
The average mean free path within the skin depth	ℓ_δ

Resonance Frequency Shift Measurement

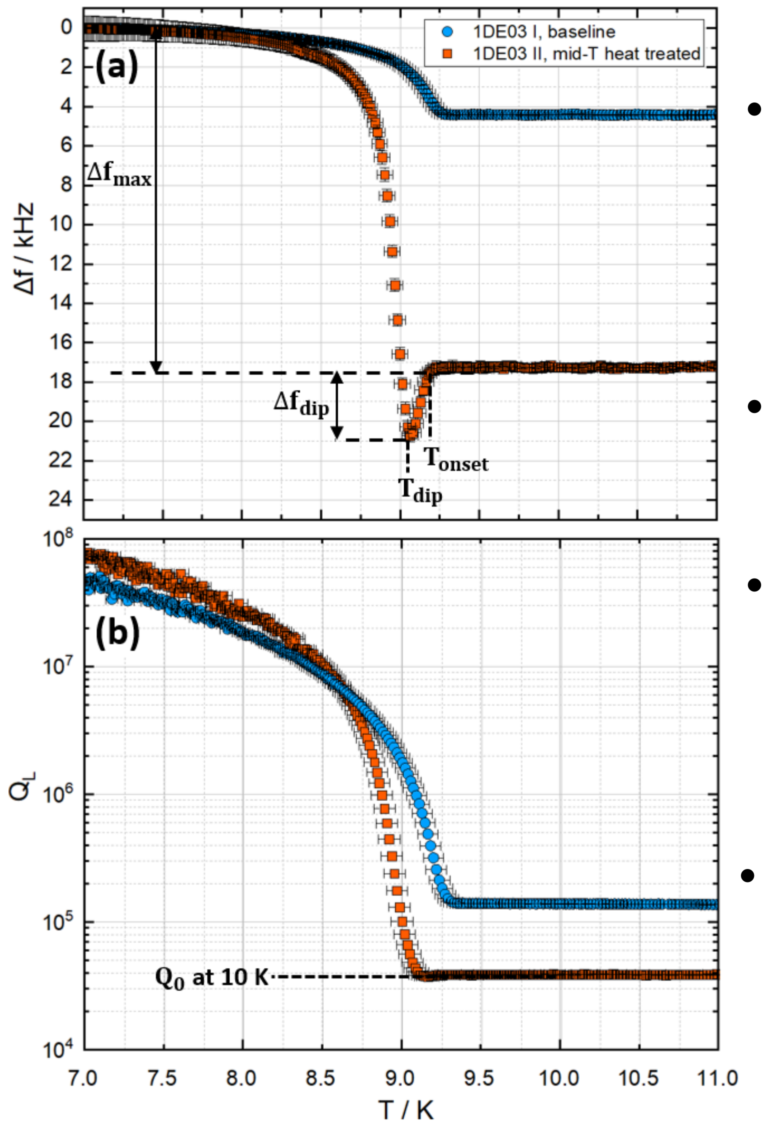

- $$\frac{\Delta f}{f} = -\frac{f\mu_0\Delta\lambda}{2G},$$
  $$\lambda(T) = \frac{\lambda_0}{\sqrt{1-\left(\frac{T}{T_c}\right)^4}}, \lambda_0 = \lambda_L\sqrt{1+\frac{\pi\xi_0}{2\ell}}$$
  → The total penetration depth $\Delta\lambda_{max}$; The average mean free path within the total penetration depth ℓ_λ
- Dip phenomenon
  → The dip magnitude Δf_{dip}; The dip width $T_{onset} - T_{dip}$
- $$Q_0 = \frac{G}{R_s}, Q_0(10\ K) \cong Q_L(10\ K),$$
  $$\rho\ell_{Nb} = 3.7\times10^{-16}\ \Omega m^2$$
  [E. L. Garwin, et al., 1972, Resistivity Ratio of Niobium Superconducting Cavities]
  → The normal conducting skin depth δ; The average mean free path within the skin depth ℓ_δ
- $$C_O = \frac{\Delta\rho}{4.5\times10^{-8}\ \Omega\cdot m\cdot at\%^{-1}}$$
  [K. K. Schulze, 1981, Preparation and Characterization of Ultra-High-Purity Niobium]

The total penetration depth	$\Delta\lambda_{max}$
The average mean free path within the total penetration depth	ℓ_λ
The dip magnitude	Δf_{dip}
The dip width	$T_{onset} - T_{dip}$
The normal conducting skin depth	δ
The average mean free path within the skin depth	ℓ_δ

Resonance Frequency Shift Measurement

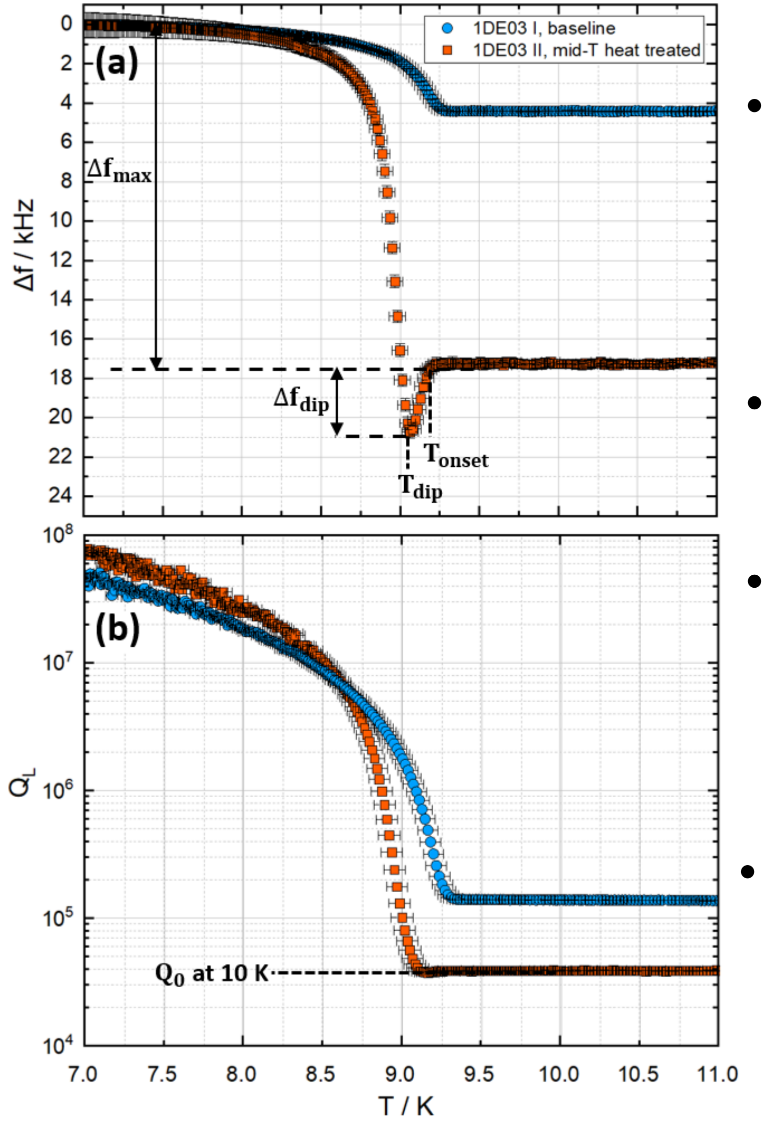

- $$\frac{\Delta f}{f} = -\frac{f \mu_0 \Delta\lambda}{2G},$$
  $$\lambda(T) = \frac{\lambda_0}{\sqrt{1-\left(\frac{T}{T_c}\right)^4}}, \lambda_0 = \lambda_L \sqrt{1 + \frac{\pi \xi_0}{2\ell}}$$
- Dip phenomenon
- $$Q_0 = \frac{G}{R_s}, Q_0(10\ K) \cong Q_L(10\ K),$$
  $$\rho \ell_{Nb} = 3.7 \times 10^{-16}\ \Omega m^2$$
  [E. L. Garwin, et al., 1972, Resistivity Ratio of Niobium Superconducting Cavities]
- $$C_O = \frac{\Delta\rho}{4.5\times10^{-8}\ \Omega{\cdot}m{\cdot}at\%^{-1}}$$
  [K. K. Schulze, 1981, Preparation and Characterization of Ultra-High-Purity Niobium]

→ The total penetration depth	$\Delta\lambda_{max}$
The average mean free path within the total penetration depth	ℓ_λ
→ The dip magnitude	Δf_{dip}
The dip width	$T_{onset} - T_{dip}$
→ The normal conducting skin depth	δ
The average mean free path within the skin depth	ℓ_δ
→ The average oxygen concentration within the total penetration depth	$c_{O,\lambda}$
The average oxygen concentration within the skin depth	$c_{O,\delta}$

A Scenario Illustrating a Simplified Oxygen Profile Using Two Data Points

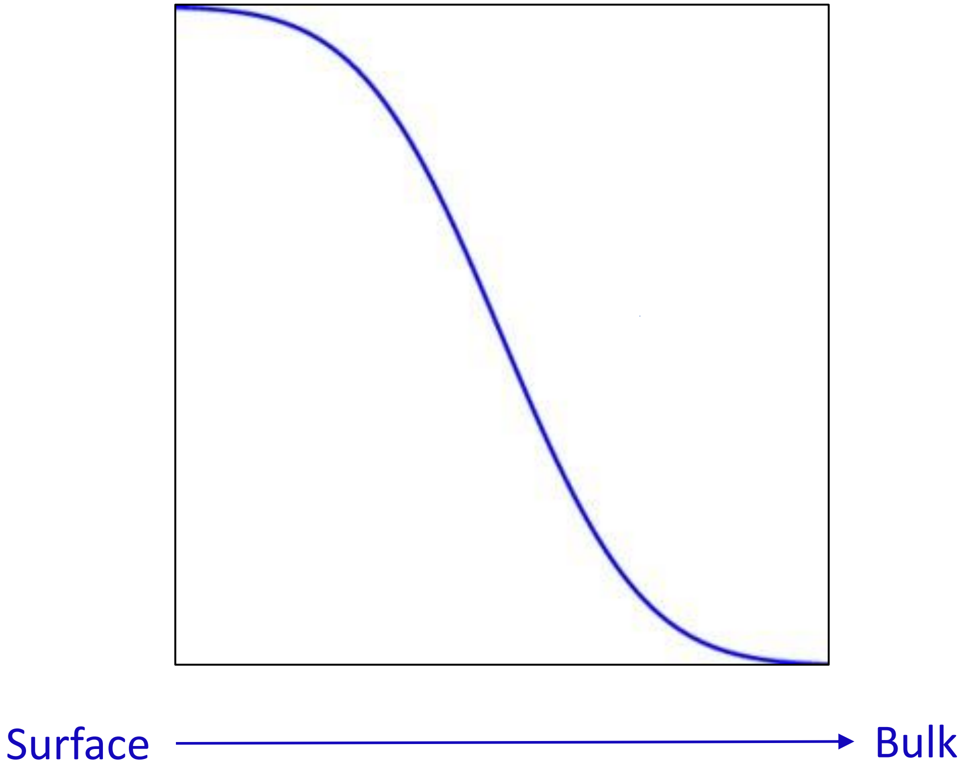

A Scenario Illustrating a Simplified Oxygen Profile Using Two Data Points

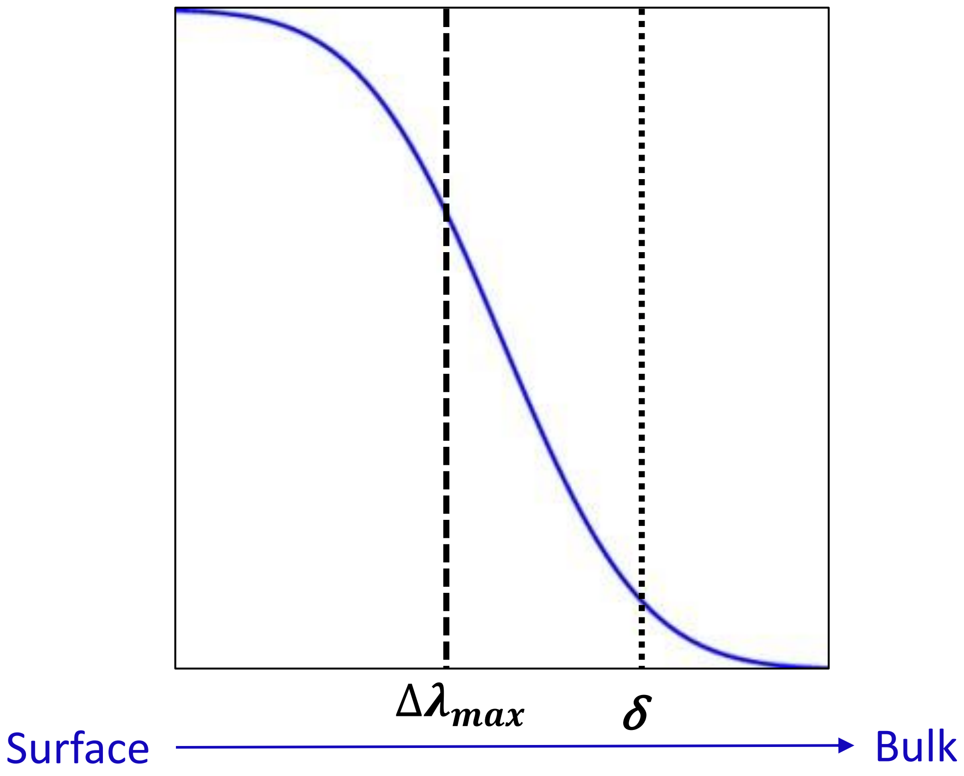

$\Delta\lambda_{max}$: The total magnetic field penetration depth

δ : The normal conducting skin depth

A Scenario Illustrating a Simplified Oxygen Profile Using Two Data Points

$c_{O,\lambda}$: Average oxygen concentration within the total magnetic field penetration depth

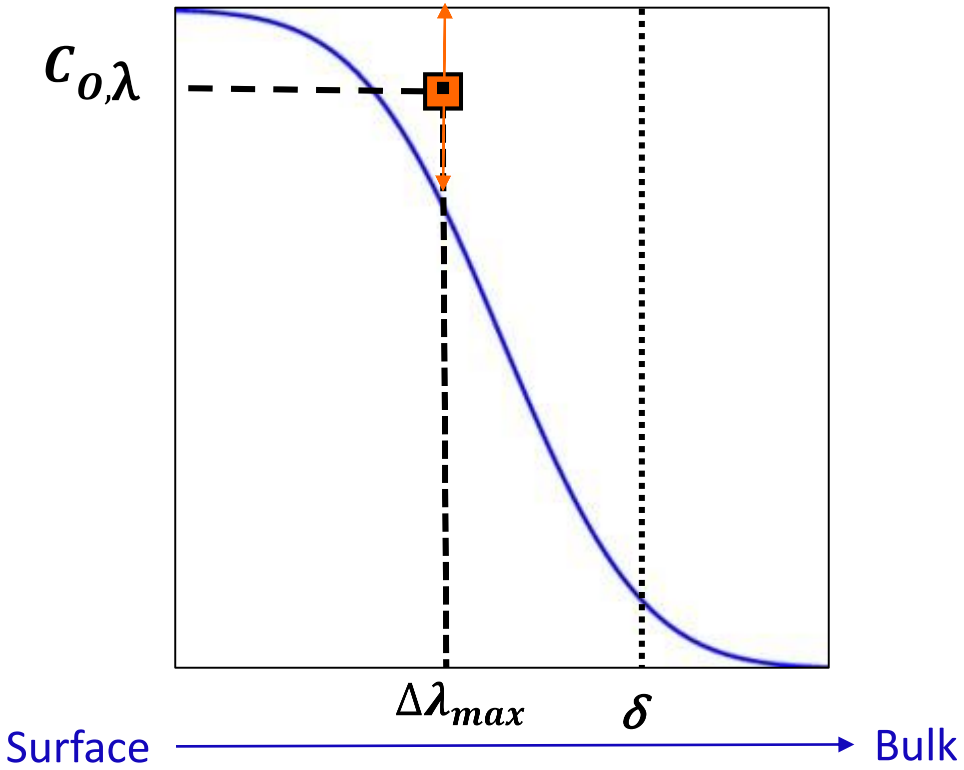

$\Delta\lambda_{max}$: The total magnetic field penetration depth

δ : The normal conducting skin depth

A Scenario Illustrating a Simplified Oxygen Profile Using Two Data Points

$c_{O,\lambda}$: Average oxygen concentration within the total magnetic field penetration depth

$c_{O,\delta}$: Average oxygen concentration within the normal conducting skin depth

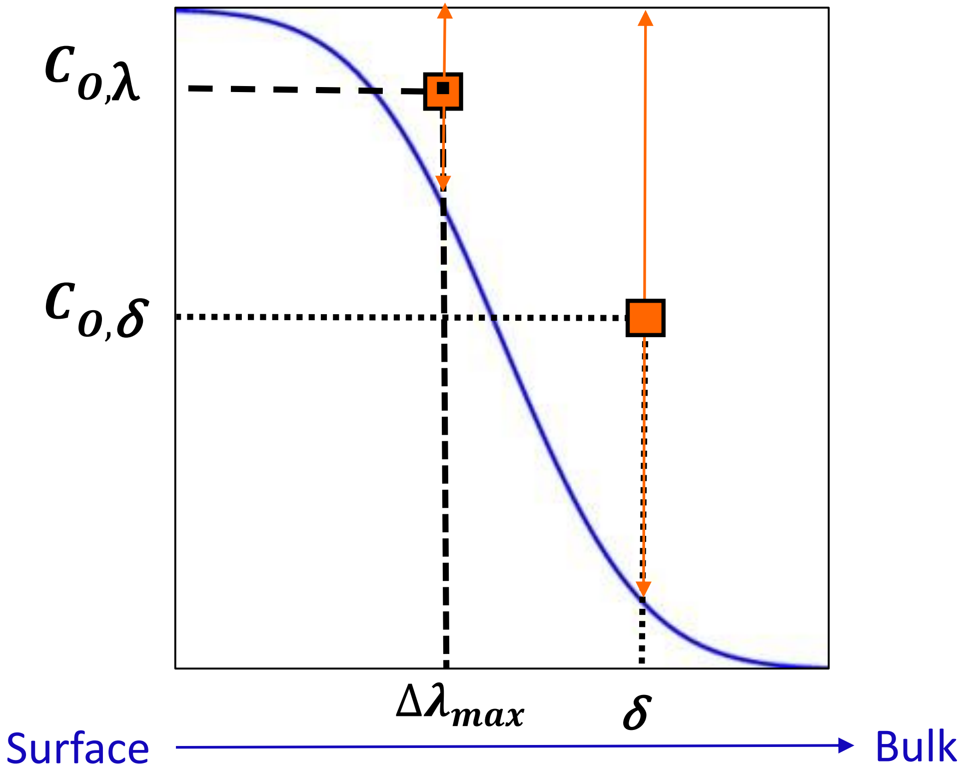

$\Delta\lambda_{max}$: The total magnetic field penetration depth

δ : The normal conducting skin depth

A Scenario Illustrating a Simplified Oxygen Profile Using Two Data Points

$c_{O,\lambda}$: Average oxygen concentration within the total magnetic field penetration depth

$c_{O,\delta}$: Average oxygen concentration within the normal conducting skin depth

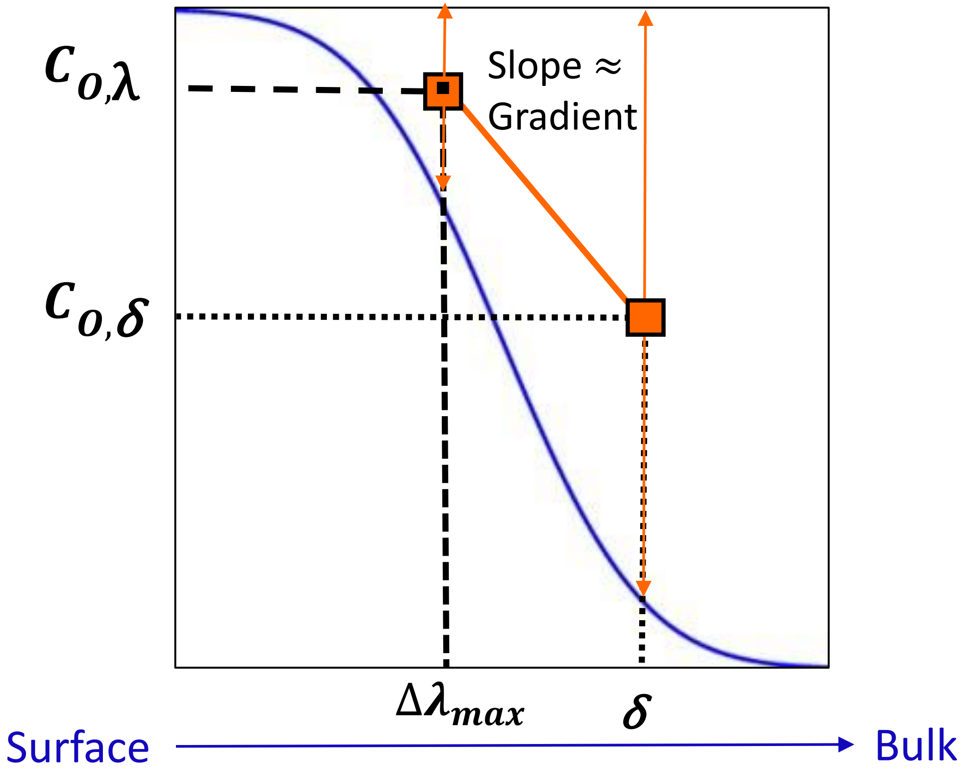

$\Delta\lambda_{max}$: The total magnetic field penetration depth

δ : The normal conducting skin depth

A Scenario Illustrating a Simplified Oxygen Profile Using Two Data Points

$c_{O,\lambda}$: Average oxygen concentration within the total magnetic field penetration depth

$c_{O,\delta}$: Average oxygen concentration within the normal conducting skin depth

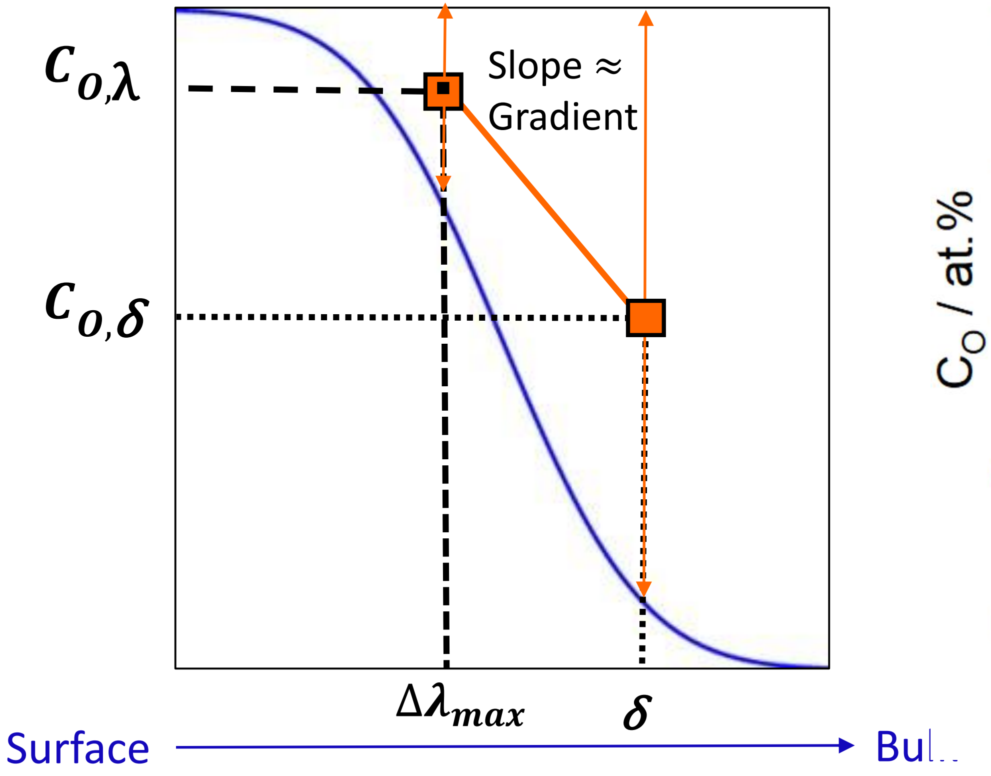

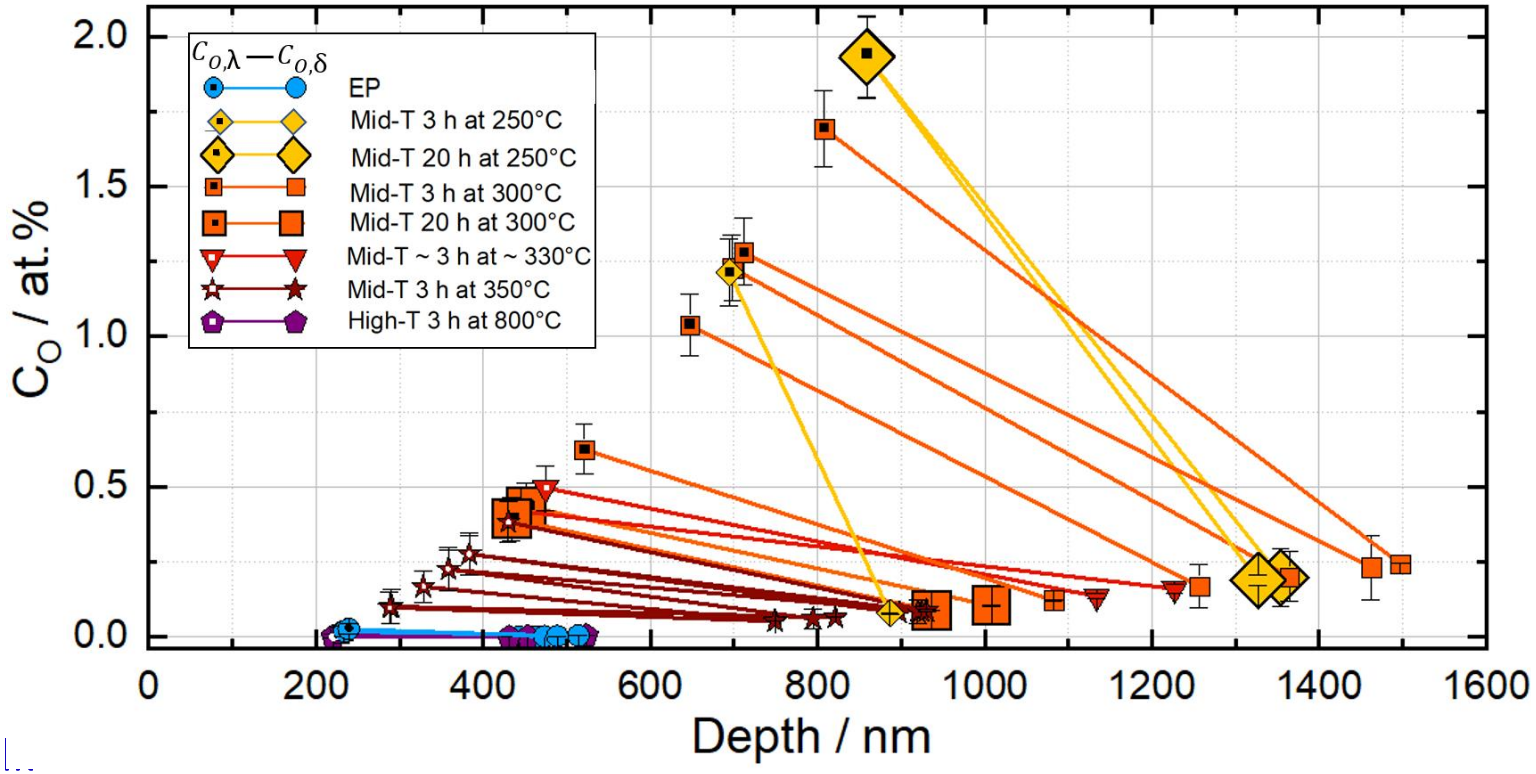

$\Delta\lambda_{max}$: The total magnetic field penetration depth

δ : The normal conducting skin depth

Gradient of Oxygen Profile Strongly Depends on Heating Temperature

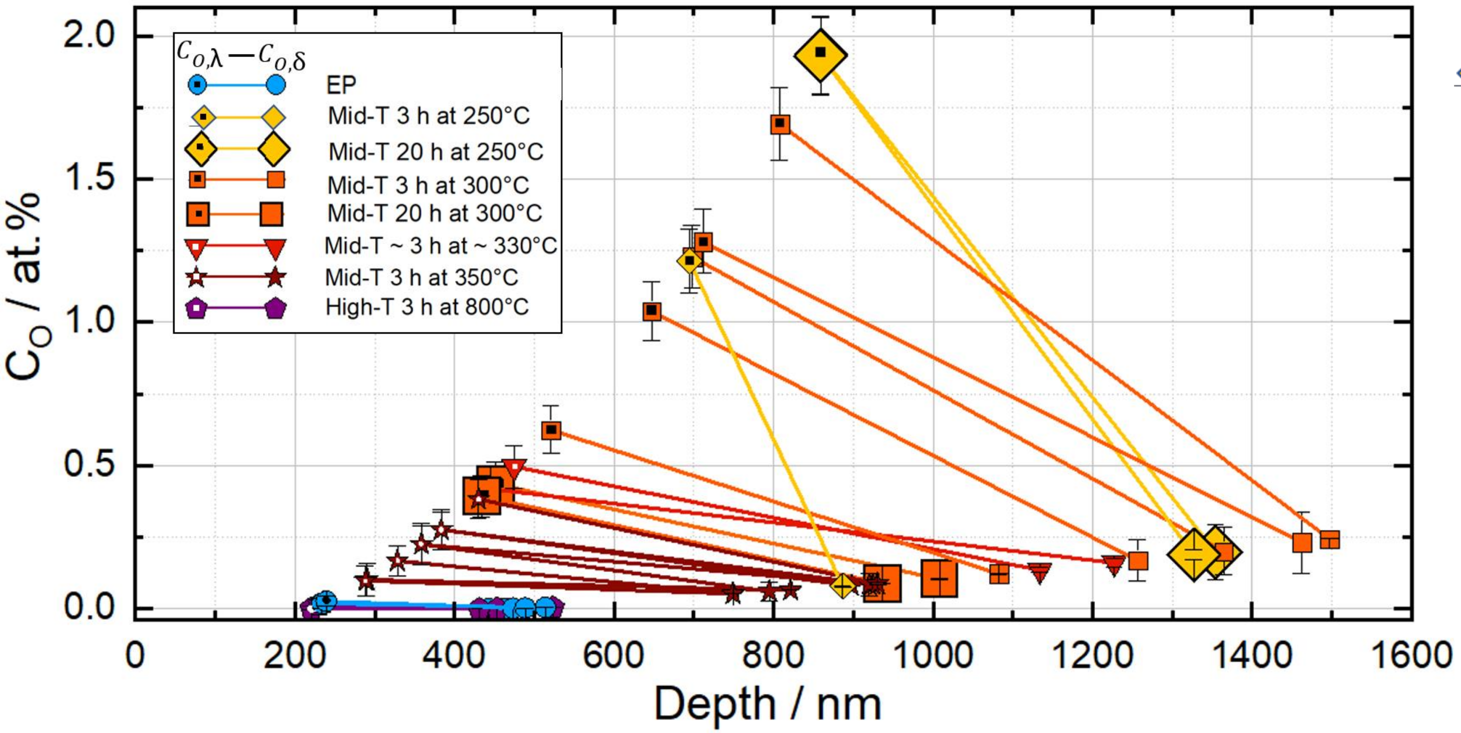

 Highest gradient accurs for 3 h at 250°C

HELMHOLTZ
Bundesministerium für Bildung und Forschung
Universität Hamburg
DER FORSCHUNG | DER LEHRE | DER BILDUNG
DESY.

Gradient of Oxygen Profile Strongly Depends on Heating Temperature

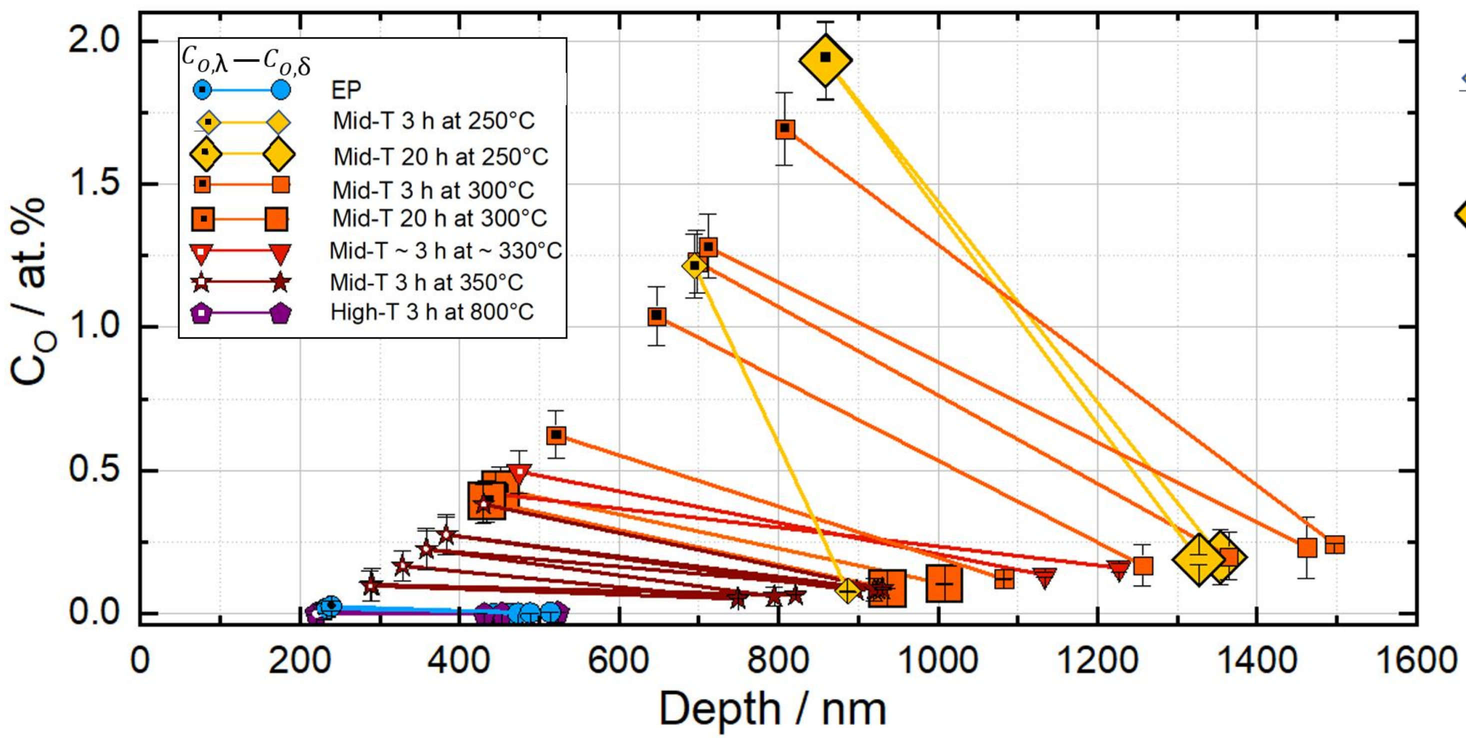

 Highest gradient accurs for 3 h at 250°C

 For 20 h at 250°C, gradient remains high

Gradient of Oxygen Profile Strongly Depends on Heating Temperature

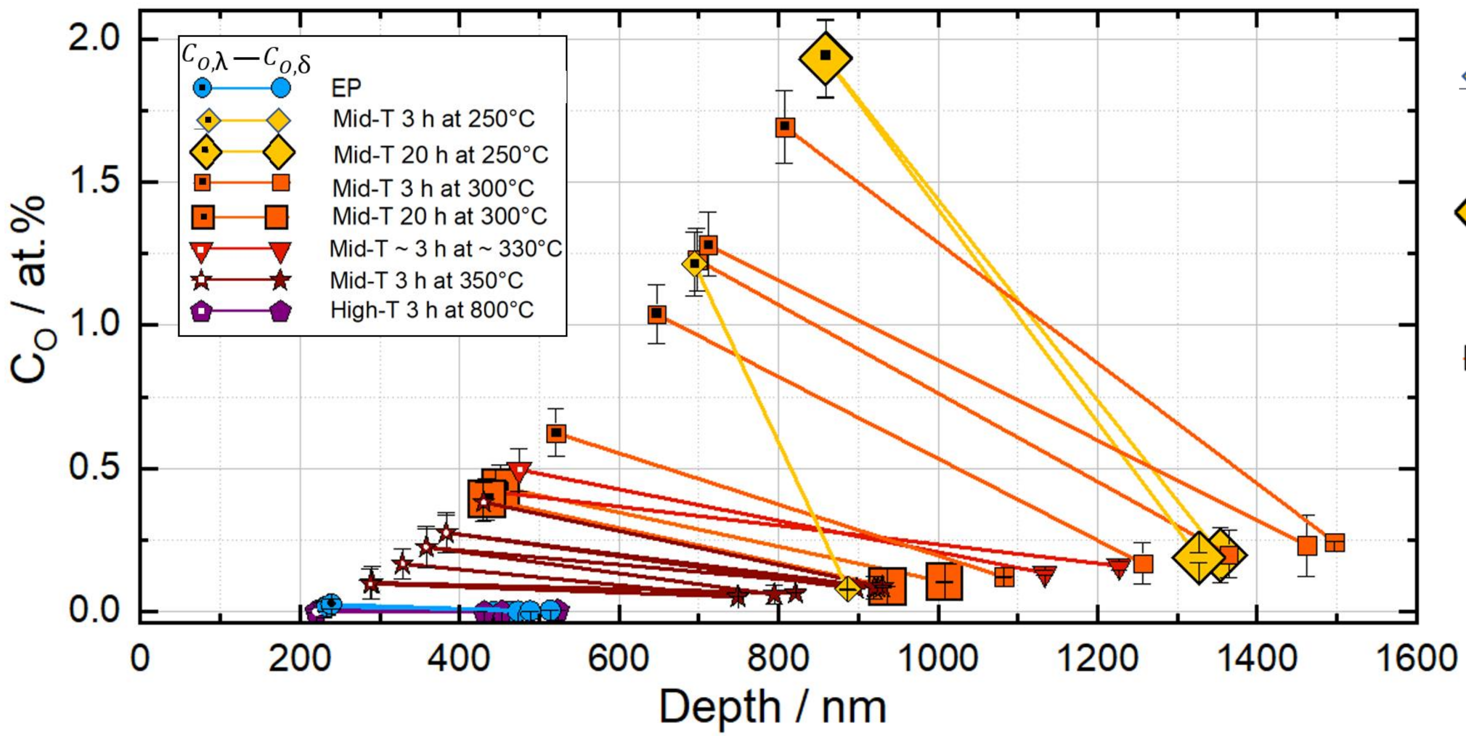

- Highest gradient accurs for 3 h at 250°C
- For 20 h at 250°C, gradient remains high
- Cavities treated for 3 h at 300°C: a comparable gradient, yet covering a wide range of C_O values

HELMHOLTZ Bundesministerium für Bildung und Forschung Universität Hamburg DER FORSCHUNG | DER LEHRE | DER BILDUNG DESY.

Gradient of Oxygen Profile Strongly Depends on Heating Temperature

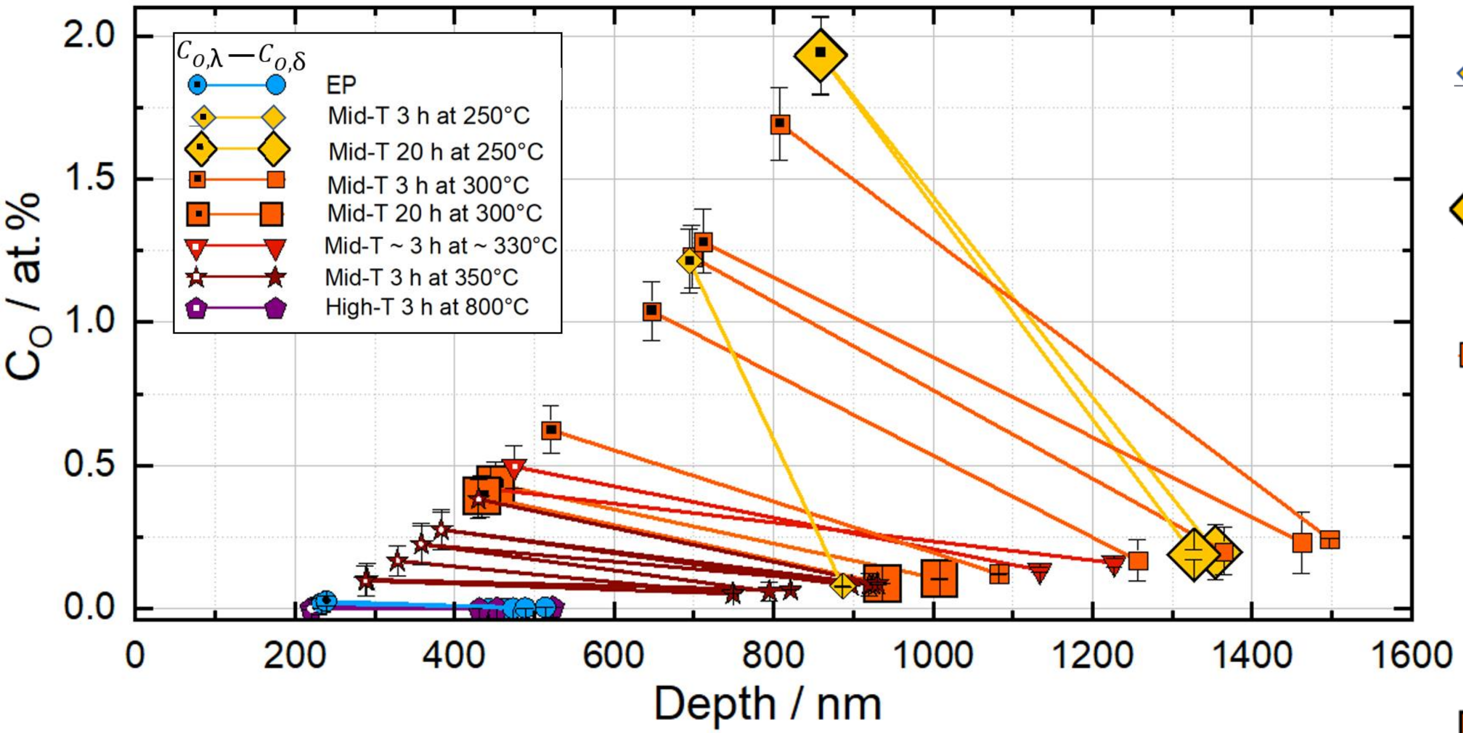

- Highest gradient accurs for 3 h at 250°C
- For 20 h at 250°C, gradient remains high
- Cavities treated for 3 h at 300°C: a comparable gradient, yet covering a wide range of C_O values
- Gradient sharply decreases at higher T or for longer t than 3 h at 300°C

Dip Width in Agreement with T_c Suppression of Nb Due to Adding O Interstitials

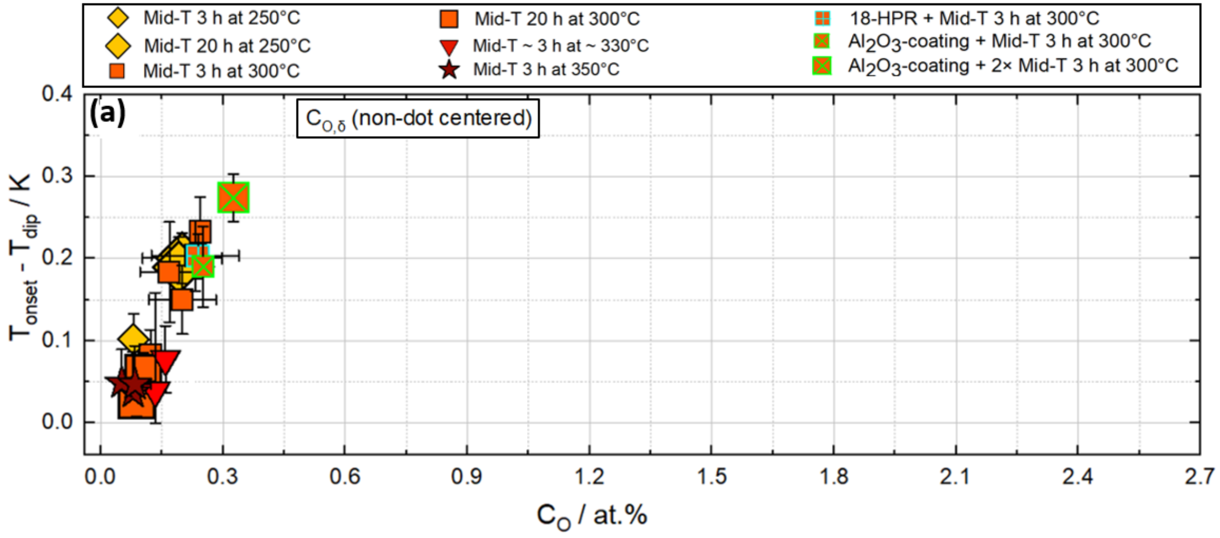

- $T_{onset} - T_{dip}$ vs. $C_{O,\delta}$, strong linear relationship

Dip Width in Agreement with T_c Suppression of Nb Due to Adding O Interstitials

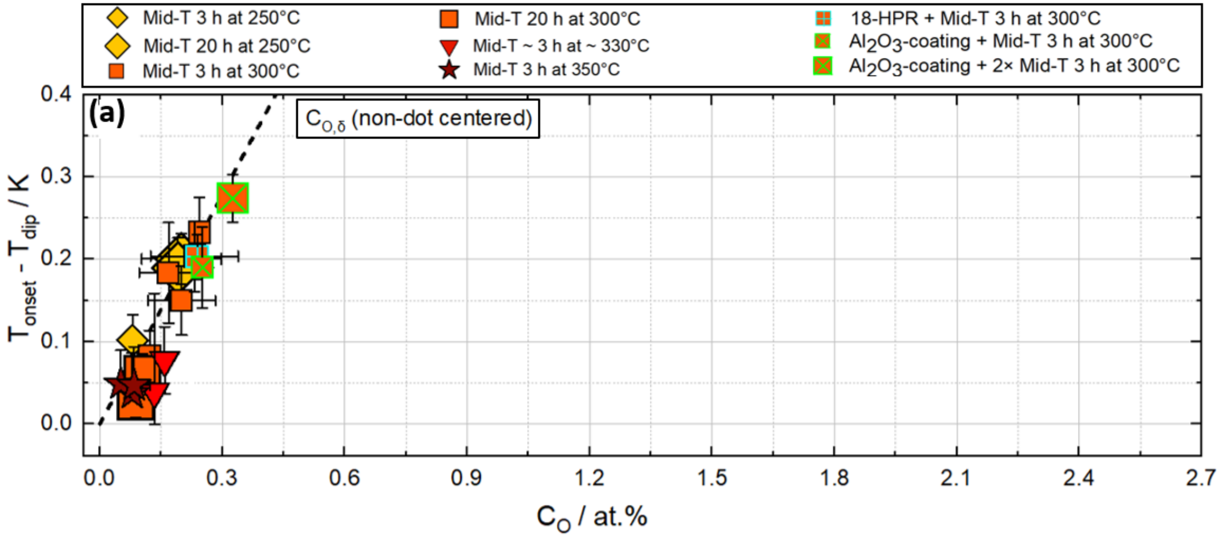

- $T_{onset} - T_{dip}$ vs. $C_{O,\delta}$, strong linear relationship

- - - [W. Desorbo, 1963, Effect of Dissolved Gases on Some Superconducting Properties of Niobium]

Dip Width in Agreement with T_c Suppression of Nb Due to Adding O Interstitials

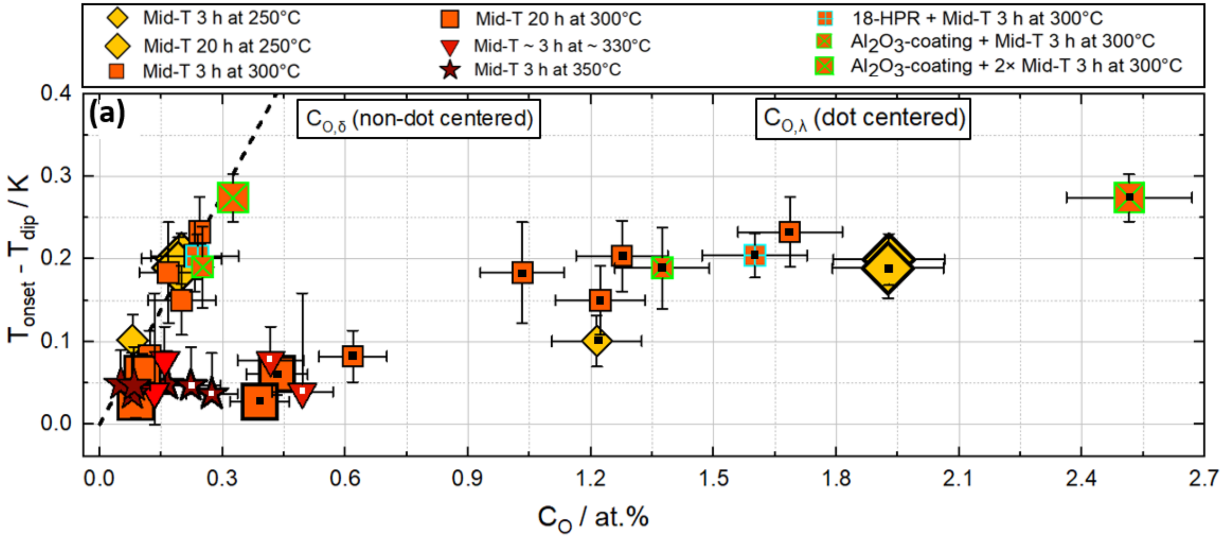

- $T_{onset} - T_{dip}$ vs. $C_{O,\delta}$, strong linear relationship
- $T_{onset} - T_{dip}$ vs. $C_{O,\lambda}$, weaker linear or logaritmic dependence

- - - [W. Desorbo, 1963, Effect of Dissolved Gases on Some Superconducting Properties of Niobium]

Dip Width in Agreement with T_c Suppression of Nb Due to Adding O Interstitials

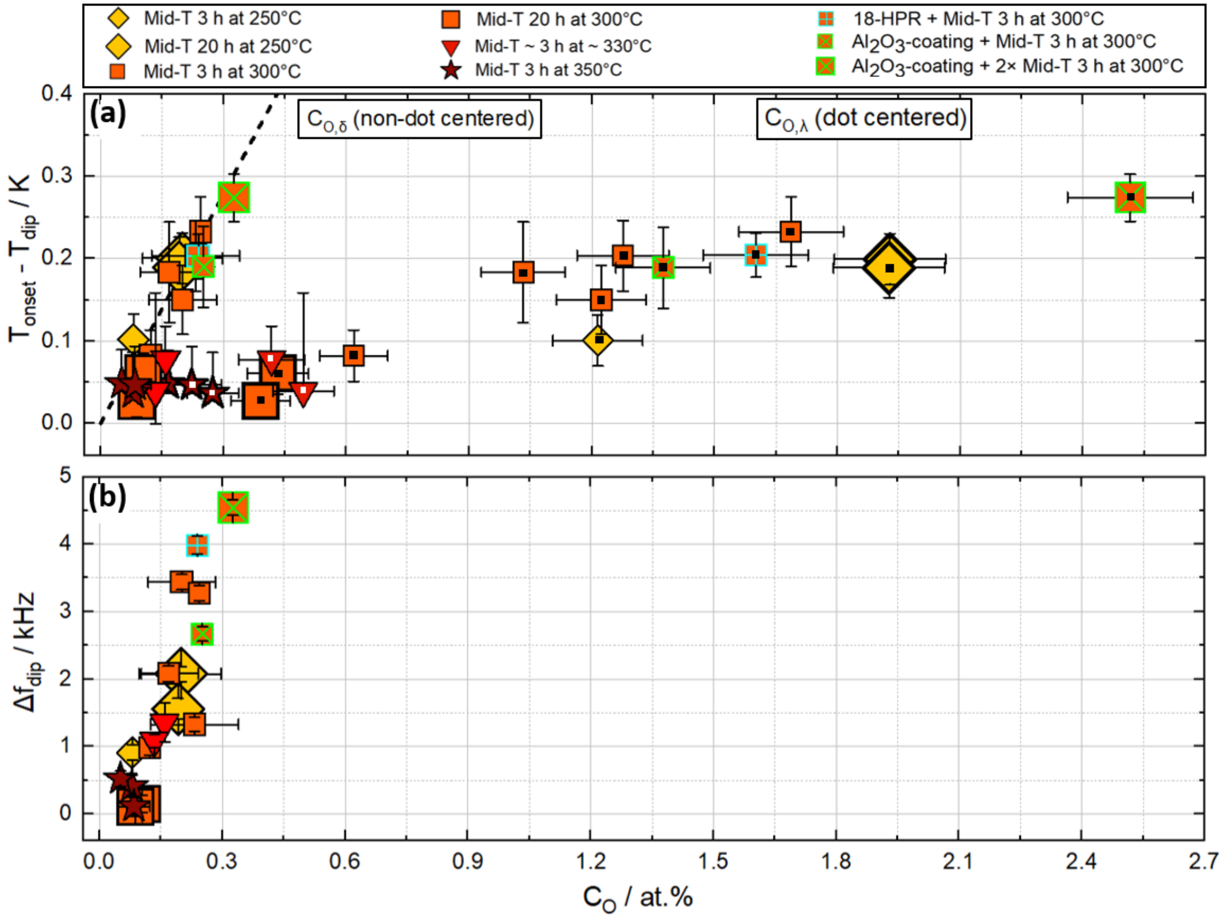

- - - [W. Desorbo, 1963, Effect of Dissolved Gases on Some Superconducting Properties of Niobium]

- $T_{onset} - T_{dip}$ vs. $C_{O,\delta}$, strong linear relationship
- $T_{onset} - T_{dip}$ vs. $C_{O,\lambda}$, weaker linear or logaritmic dependence
- Δf_{dip} vs. $C_{O,\delta}$, strong linear relationship

Dip Width in Agreement with T_c Suppression of Nb Due to Adding O Interstitials

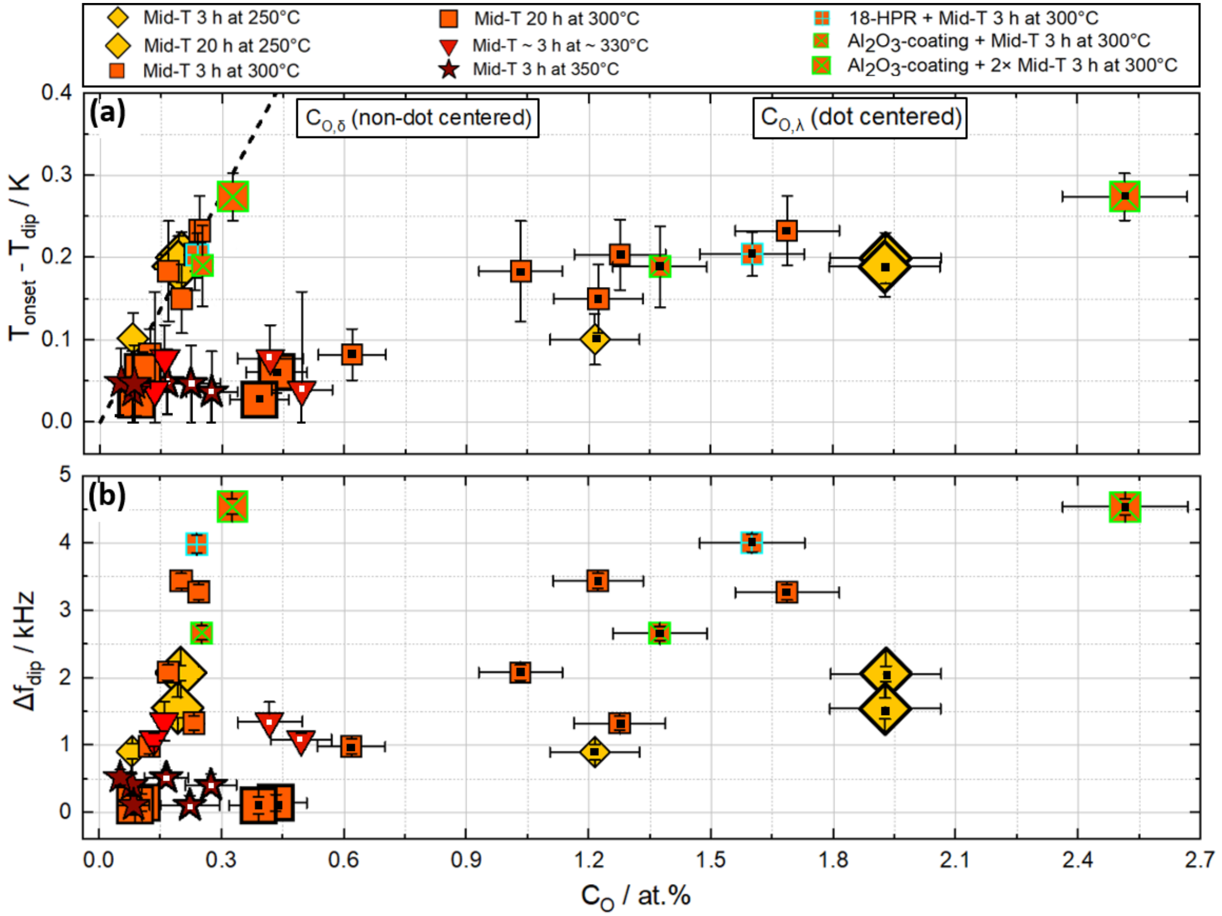

- - - [W. Desorbo, 1963, Effect of Dissolved Gases on Some Superconducting Properties of Niobium]

- $T_{onset} - T_{dip}$ vs. $C_{O,\delta}$, strong linear relationship
- $T_{onset} - T_{dip}$ vs. $C_{O,\lambda}$, weaker linear or logaritmic dependence
- Δf_{dip} vs. $C_{O,\delta}$, strong linear relationship
- Δf_{dip} vs. $C_{O,\lambda}$, weak, highly scattered relationship, especially for 250°C treatments

Conclusion

- Mid-T heat treatments produce strongly temperature-dependent oxygen-gradient profiles

Conclusion

- Mid-T heat treatments produce strongly temperature-dependent oxygen-gradient profiles
- Mid-T heat treatments at 250 °C results in a markedly high gradient, and extending the duration from 3 h to 20 h does not substantially reduce it

Conclusion

- Mid-T heat treatments produce strongly temperature-dependent oxygen-gradient profiles
- Mid-T heat treatments at 250 °C results in a markedly high gradient, and extending the duration from 3 h to 20 h does not substantially reduce it
- Mid-T heat treatments ≥330 °C for ≥3 h generate an oxygen distribution with a relatively low gradient

HELMHOLTZ Bundesministerium für Bildung und Forschung Universität Hamburg DER FORSCHUNG | DER LEHRE | DER BILDUNG DESY.

Conclusion

- Mid-T heat treatments produce strongly temperature-dependent oxygen-gradient profiles
- Mid-T heat treatments at 250 °C results in a markedly high gradient, and extending the duration from 3 h to 20 h does not substantially reduce it
- Mid-T heat treatments ≥330 °C for ≥3 h generate an oxygen distribution with a relatively low gradient
- The dip width—that is, the temperature interval from the onset of the dip to its minimum—reflects the Tc suppression caused by interstitial oxygen

Conclusion

- Mid-T heat treatments produce strongly temperature-dependent oxygen-gradient profiles
- Mid-T heat treatments at 250 °C results in a markedly high gradient, and extending the duration from 3 h to 20 h does not substantially reduce it
- Mid-T heat treatments ≥330 °C for ≥3 h generate an oxygen distribution with a relatively low gradient
- The dip width—that is, the temperature interval from the onset of the dip to its minimum—reflects the Tc suppression caused by interstitial oxygen
- The dip correlates more strongly with the average oxygen concentration within the normal-conducting skin depth than with the average oxygen concentration within the total magnetic-field penetration depth

Thank you for your attention!

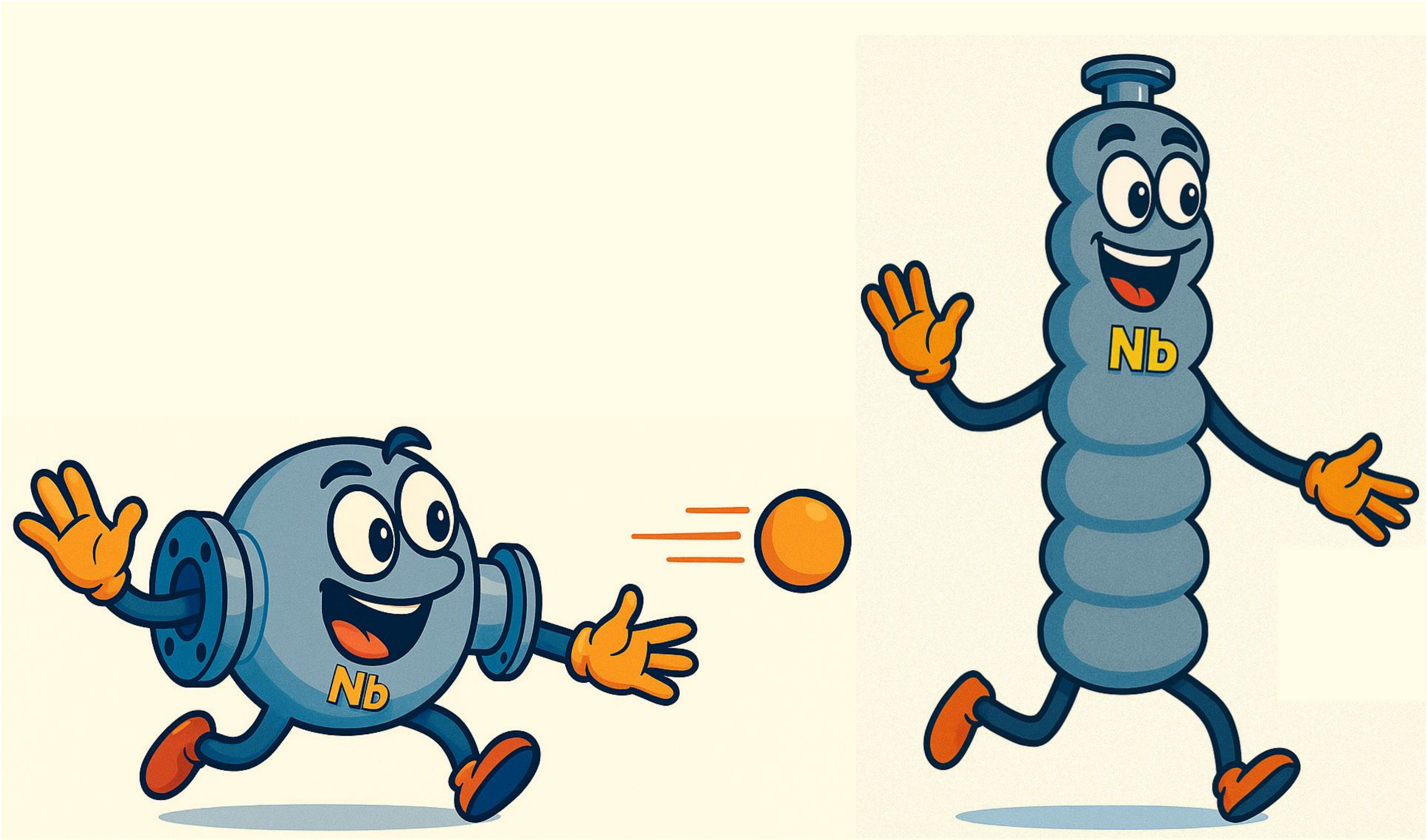

Created by Rezvan and AI

Contact

Deutsches Elektronen-
Synchrotron DESY
www.desy.de

Rezvan Ghanbari
Institute of Experimental Physics
University of Hamburg
E-mail: rezvan.ghanbari@desy.de
Phone: (+49) 040-8998-4321